Vol. 426: 119–131, 2011
doi: 10.3354/meps09000

MARINE ECOLOGY PROGRESS SERIES
Mar Ecol Prog Ser

Published March 28

Non-photochemical quenching of chlorophyll fluorescence and xanthophyll cycle responses after excess PAR and UVR in *Chaetoceros brevis*, *Phaeocystis antarctica* and coastal Antarctic phytoplankton

Willem H. van de Poll[1,2,*], Marcos Lagunas[3,4], Tea de Vries[1], Ronald J. W. Visser[1], Anita G. J. Buma[1]

[1]Department of Ocean Ecosystems, Energy and Sustainability Research Institute, University of Groningen, PO Box 14, 9750 AA Haren, The Netherlands
[2]Royal Netherlands Institute for Sea Research, PO Box 59, 1790 AB Den Burg (Texel), The Netherlands
[3]Estación de Fotobiología Playa Unión, Rawson, Playa Unión, Casilla de Correos No. 15, 9103 Chubut, Argentina
[4]Department of Biology, University of Victoria, PO Box 3020, Victoria, British Columbia, V8W 3N5, Canada

ABSTRACT: Sensitivity to photoinhibition from near-surface irradiance was determined in coastal phytoplankton from Potter Cove (King George Island, Antarctica) in relation to hydrographic conditions shaped by summertime meltwater influx. Slow (indicative for PSII damage) and fast (indicative for xanthophyll cycle activity) relaxing non-photochemical chlorophyll fluorescence quenching (NPQ) was measured during recovery from excess photosynthetically active radiation (PAR) and PAR + ultraviolet radiation (UVR) for 3 stations differentially affected by sediment influx. Additionally, assemblages were incubated outside to study xanthophyll cycle activity during PAR and PAR+UVR exposure. For comparison, NPQ and xanthophyll cycle activity were determined for high (125 µmol photons m^{-2} s^{-1}) and low (20 µmol photons m^{-2} s^{-1}) light acclimated *Chaetoceros brevis* (Bacillariophyceae) and *Phaeocystis antarctica* (Haptophyceae) cultures. Pigment analysis (CHEMTAX) revealed diatom dominance (average 74%) at all locations, with haptophytes being of minor importance (average 13%). All stations were stratified by a vertical density gradient, whereas sediment influx was significantly higher at the innermost station. Taxonomic composition, NPQ characteristics, and photoprotective pigment ratios were not different among stations. At the chlorophyll maximum, phytoplankton showed high light acclimation at all locations, and fast relaxing NPQ dominated after excess PAR and PAR+UVR. Samples from below the chlorophyll maximum were enriched in haptophytes, showed lower photoprotective pigment ratios, reduced capacity for NPQ, and increased contribution of slow relaxing NPQ. The photoprotective capacity of high and low light acclimated *C. brevis* and *P. antarctica* differed significantly. *P. antarctica* induced less NPQ and there was a stronger slow relaxing NPQ component than in the diatom, particularly after low light acclimation. Although total NPQ decreased and slow relaxing NPQ increased after UVR in field samples, NPQ and the xanthophyll cycle de-epoxidation state of cultures were not affected by UVR. A higher photoprotective capacity of diatoms over haptophytes may explain their dominance in stratified meltwater-affected coastal Antarctic waters.

KEY WORDS: Antarctic phytoplankton · Chlorophyll fluorescence · Non-photochemical quenching · Photoacclimation · Ultraviolet radiation · Xanthophyll cycle

INTRODUCTION

Low iron availability and light limitation due to deep vertical mixing are considered the main factors constraining phytoplankton growth in the open Southern Ocean, leaving high macronutrient concentrations that are not exploited by phytoplankton growth (van Oijen et al. 2004a). Although phytoplankton rarely reaches concentrations in excess of 5 mg chlorophyll *a* (chl *a*) m^{-3}, there can be considerable variation in chlorophyll

*Email: w.h.van.de.poll@rug.nl

biomass on a temporal and spatial scale. These differences have been primarily attributed to elevated iron concentrations due to natural iron fertilization and to differences in mixed layer depths (De Baar et al. 2005, Blain et al. 2007). Deep mixed layers can extend below the euphotic zone, thereby reducing phytoplankton light exposure. A stabilization of the mixed layer (stratification) can be induced by elevated temperature and by the influx of fresh water.

Limitation of summer time phytoplankton accumulation (~0.2 to 0.4 mg chl *a* m^{-3}) due to low iron availability (~0.33 nM Fe l^{-1}) and deep mixed layers (upper mixed layer, UML, at ~80 m) has been observed in the Drake Passage (Hewes et al. 2009, A. C. Alderkamp et al. unpubl.). In contrast, the Bransfield Strait and the waters surrounding the South Shetland Islands (SSI) have relatively high iron concentrations that originate from the Weddell Sea (~3.0 nM Fe l^{-1}; Hewes et al. 2008). Here, deep mixed layers (UML at 100 to 40 m) are believed to limit summertime phytoplankton accumulation (0.5 to 1.2 mg chl *a* m^{-3}). Seasonally released meltwater (from sea ice, glaciers, and rivers) along the SSI alters the hydrography of coastal waters as in other regions in the West Antarctic Peninsula area (Dierssen et al. 2002). Stratification of the water column provides phytoplankton with a more stable light environment, which allows utilization of the stronger light closer to the water surface, thereby enhancing growth rates. More than 10 yr of monitoring in Potter Cove (King George Island, SSI) has demonstrated increased meltwater input in coastal waters, which decreases surface salinity and increases sediment concentrations (Schloss et al. 2008). Despite enhanced summer stratification, phytoplankton does not reach concentrations in excess of 3.5 mg chl *a* m^{-3} in this area (Schloss & Ferreyra 2002, Schloss et al. 2002). Several mesocosm studies indicated that phytoplankton potentially can reach concentrations in excess of 10 mg chl *a* m^{-3} (Agustí & Duarte 2000, Helbling et al. 1995). This discrepancy has been attributed to the combination of stratification and high turbidity in the SSI area (Schloss & Ferreyra 2002). Recently, evidence for a role of photoinhibition in controlling phytoplankton productivity in the open Southern Ocean has been found (Alderkamp et al. 2010). Antarctic algal photosynthesis saturates at around 100 µmol photons m^{-2} s^{-1}, but radiation in excess of 1000 µmol photons m^{-2} s^{-1} can be experienced near the water surface. Algae show considerable plasticity in acclimation potential to irradiance changes (Van de Poll et al. 2007, Van de Poll & Buma 2009, Kropuenske et al. 2009). This not only influences the irradiance range that supports growth but also affects the sensitivity of species towards extremes that can occur in their environment such as excess photosynthetically active radiation (PAR) and ultraviolet radiation (UVR: 280 to 400 nm). Genetically fixed differences in photoacclimation potential have been suggested to contribute to the success of individual species under prevailing conditions (Strzepek & Harrison 2004, Lavaud et al. 2007, Dimier et al. 2009). The xanthophyll cycle is believed to be a crucial adaptation to a fluctuating light environment because it responds on a time scale of seconds to minutes to protect Photosystem II (PSII) during periodic overexcitation of photosynthetic electron transport. When exposed to excess light, a photoprotective process (NPQ: nonphotochemical quenching of chlorophyll fluorescence) is induced by acidification of the thylakoid lumen. This triggers the xanthophyll cycle (the reversible enzymatic conversion of epoxy-xanthophyll into deepoxidated xanthophyll), enhancing energy dissipation in the form of heat (Goss & Jakob 2010). As a result, excitation pressure of photosynthetic electron transport is reduced and PSII damage and metabolically costly PSII repair is limited (Van de Poll & Buma 2009). The xanthophyll cycle in diatoms and haptophytes (the diadinoxanthin cycle) differs significantly from the xanthophyll cycle in green plants. Compared to the viola-anthera-zeaxanthin cycle from plants, deepoxidation of diadinoxanthin (Dd) to diatoxanthin (Dt) occurs at higher pH, and NPQ is directly related to Dt and independent of a proton gradient (Goss et al. 2006). Furthermore, epoxidation of Dt is significantly faster than that of zeaxanthin. However, little is known about the effectiveness of NPQ and the xanthophyll cycle in phytoplankton under natural conditions and how this is influenced by other stressors such as UVR. UVR in the upper part of the water column has been found to enhance photoinhibition in phytoplankton (Fritz et al. 2008). This is of particular importance in the Antarctic where stratospheric ozone depletion increases UVBR (280 to 315 nm) during the austral spring (Arrigo 1994). UVR-induced photoinhibition has been associated with enhanced damage to the D1 reaction centre binding protein (Larkum et al. 2001). In addition, it has been suggested that the activity of the xanthophyll cycle is affected by UVR (Van de Poll & Buma 2009, Buma et al. 2009).

In the present study we monitored dominant taxonomic groups, using pigment analysis in relation with hydrographic conditions at 3 stations in Potter Cove. These locations are differently affected by meltwater during summer (Schloss et al. 2002). Furthermore, we investigated the potential to recover from excess PAR and UVR for samples from these stations, using NPQ and xanthophyll de-epoxidation characteristics. Supporting data were obtained by studying fast and slow relaxing NPQ and xanthophyll de-epoxidation in high and low light acclimated *Chaetoceros brevis* and *Phaeocystis antarctica* cultures. We discuss whether

photoinhibition provides an explanation for taxon dominance and the moderate phytoplankton biomass that is found in coastal waters of the SSI during summer.

MATERIALS AND METHODS

Field sampling King George Island. Phytoplankton samples were obtained between 15 January and 7 February 2009 from Potter Cove (62° 14′ S, 58° 38′ W, King George Island, SSI, Antarctica). A CTD (Seabird SBE 19 plus) with a Wetlab wetstar fluorescence sensor and a Licor biospherical PAR sensor was deployed from a Zodiak to a maximum depth of 100 m. CTD data were viewed onboard on a rugged notebook (Getag) and samples were collected with a 20 l Niskin bottle during the upcast. Three stations were sampled (Fig. 1): S1, located in Maxwell Bay at the entrance to Potter Cove (depth >100 m), was sampled 16 times; whereas S2 and S3, positioned inside Potter Cove (depth ~35 m), were sampled 14 and 5 times, respectively. S3 was closest to input sites of sediment-rich water from glaciers that drain into Potter Cove. In contrast, S1 represented water entering Potter Cove after cyclonic circulation in Maxwell Bay, originating from the Bransfield Strait. All stations were sampled in the morning between 9:30 and 11:00 h. The samples were collected from the chl maximum as measured from the CTD fluorescence sensor. Samples from below the chl maximum (depth 40 to 83 m, n = 6) and from the surface (n = 3) were collected on several occasions at S1. The 20 l Niskin samples were transported in plastic bags that were kept dark and cold, and were processed within 2 h after collection for pigment composition, particulate organic carbon (POC), and NPQ experiments. An overview of the experiments is presented in Fig. 2. For pigment analysis, 2 to 10 l of seawater were filtered by vacuum (0.5 mbar) onto 47 mm GF/F filters. Filters were snap frozen in liquid nitrogen and stored at −80°C until analysis. For POC analysis, aliquots of 200 to 300 ml seawater were filtered on 13 mm combusted GF/F filters and stored at −80°C until analysis. For NPQ experiments, ~1 l of sample was used.

Hydrographic data. The attenuation coefficient for PAR (K_d) was calculated from linear regression on ln-transformed irradiance data, from which the 1% depth for PAR was calculated. The chl maximum depth was determined from the CTD fluorescence sensor. The depth of the UML was defined as the first depth (from the surface) where density (sigma theta units) increased by 0.05 kg m^{-3}.

Field experiments: NPQ and xanthophyll de-epoxidation state. NPQ capacity of field samples (36 samples in total) was determined by exposing aliquots of 400 ml in quartz cuvettes to 20 min excess PAR and PAR+UVR provided from below, in a temperature-controlled set-up (1°C). Afterwards, recovery was monitored under low light (5 to 10 µmol photons m^{-2} s^{-1}) over 10 min intervals by water PAM fluorometry on 30 ml samples (see 'Analytical procedures'). The excess PAR and PAR+UVR treatments approximated near-surface irradiance (hereafter referred to as 'simulated surface irradiance'; see also Van de Poll et al. 2006). Irradiance was provided by a 250 W m^{-2} high-pressure halogen lamp (Philips Powertone) and 2 UVB fluorescent lamps (Philips TL 12, 20 W). A WG 305 glass filter (Schott) was

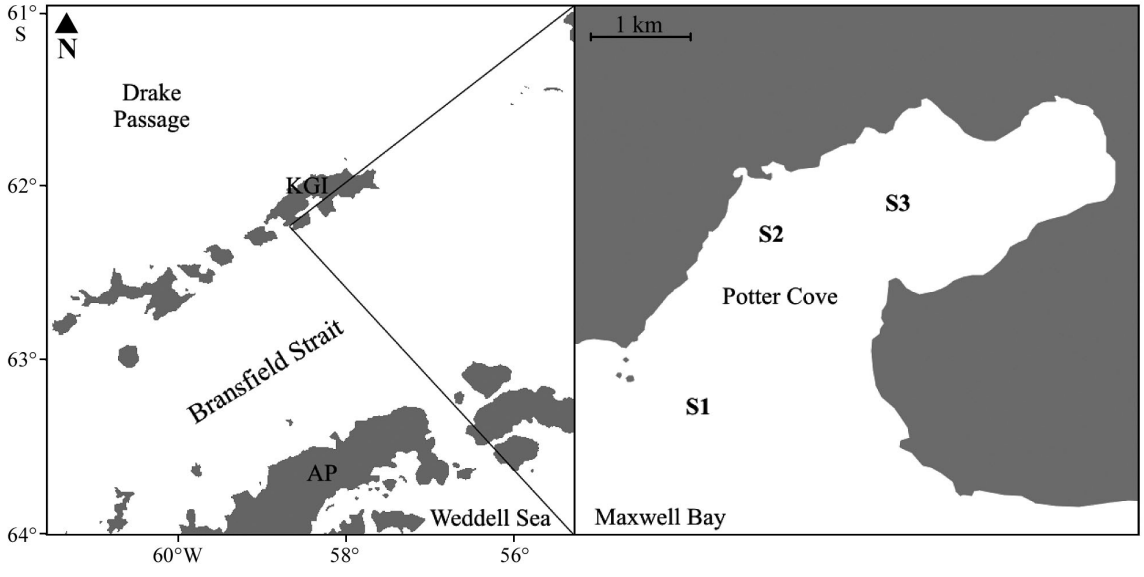

Fig. 1. Map showing South Shetland Islands (KGI: King George Island) and the Antarctic Peninsula (AP), Weddell Sea, Drake Passage, and Bransfield Strait. Inset: Maxwell Bay and Potter Cove and the locations of sampling stations S1, S2, and S3

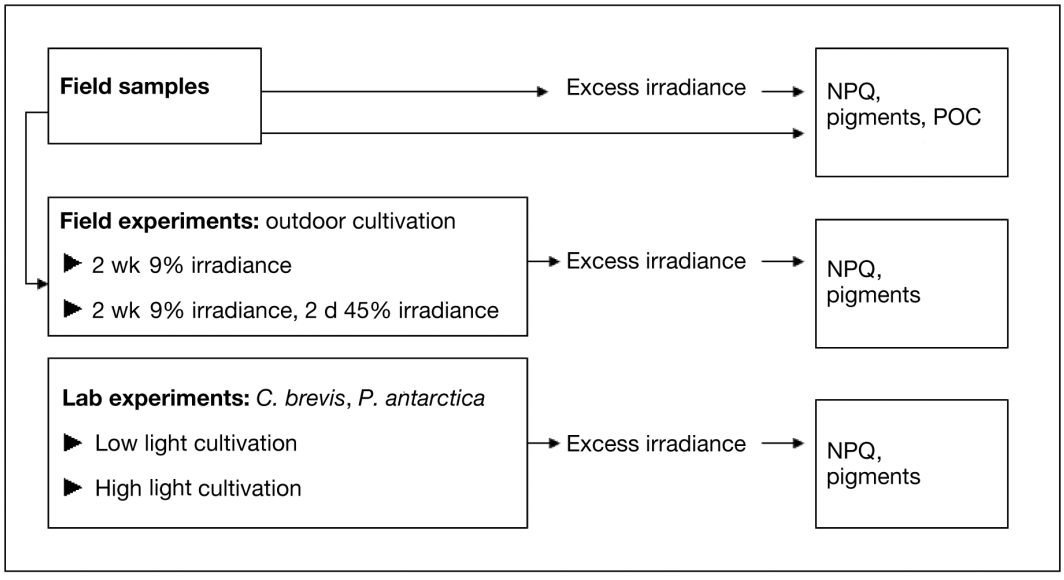

Fig. 2. Overview of the experiments performed with field samples, cultivated field samples (field experiments), and laboratory cultures of *Chaetoceros brevis* and *Phaeocystis antarctica* (lab experiments)

used to block unnatural UVBR (280 to 315 nm) and UVCR (<280 nm) from the PAR+UVR treatment, whereas a GG 385 filter (Schott) removed UVBR and short wavelength UVAR (315 to 400 nm) from the PAR treatment. Spectral irradiance was measured with a MACAM SR9910 spectroradiometer and a spherical sensor in the cuvettes. Samples subjected to excess PAR+UVR treatment received 410 W m^{-2} PAR (1900 µmol photons m^{-2} s^{-1}), 42.6 W m^{-2} UVAR, and 3.3 W m^{-2} UVBR. For the PAR treatment the amounts received were 383 W m^{-2} (1785 µmol photons m^{-2} s^{-1}) PAR, 21 W m^{-2} UVAR, and 0.19 W m^{-2} UVBR.

Xanthophyll de-epoxidation state during simulated surface irradiance could not be studied in field samples due to long filtration time (≥30 min). To increase biomass and reduce filtration time to <5 min, field samples were cultivated under semi-controlled conditions. Samples from the chl maximum of S1 were incubated in 4 transparent 5 l polypropylene bags in a seawater-cooled set-up (1 to 3°C) on shore. Natural radiation was reduced to 9% by 3 layers of black neutral density screen. After 12 d of incubation, 400 ml subsamples were exposed to simulated surface irradiance (PAR and PAR+UVR). After 0, 20, 60 and 120 min of exposure, samples (400 ml) were filtered onto 47 mm GF/F for pigment composition to investigate de-epoxidation of the xanthophyll cycle pigment (Dd). This experiment was repeated once. In another experiment, NPQ and the relaxation of the xanthophyll cycle pigments (epoxidation of Dt) were monitored after 20 min PAR and PAR+UVR exposure in low light for 90 min in aliquots of 400 ml. In this experiment, samples were taken from one bag that received 9% radiation and one bag that was exposed to higher radiation for 2 d (45% of incoming radiation, 1 layer of neutral density screen). There were no replicates in this experiment.

Lab experiments: NPQ and xanthophyll de-epoxidation. *Chaetoceros brevis* (CCMP 163) and *Phaeocystis antarctica* (CCMP 1871) were grown in F2-enriched autoclaved seawater at 4 (± 0.5)°C. Constant irradiance was provided by 12 fluorescent light tubes in a U-shaped set-up (Van de Poll et al. 2007) under a 12:12 h light:dark cycle. The cultures were grown under 125 and 20 µmol photons m^{-2} s^{-1} (referred to as high and low light, respectively). Irradiance was measured in air in the cultivation vessels with a QSL 100 equipped with a spherical sensor (Biospherical Instruments). The cultures were maintained in semi-continuous batch mode for at least 2 wk prior to the experiments.

Fluorescence measurements (see below) were performed during recovery in low light. NPQ characteristics were determined for low and high light acclimated cultures (100 ml) that were exposed to simulated surface irradiance (PAR, PAR+UVR) for 20 min and placed in low light (10 µmol photons m^{-2} s^{-1}) for recovery. These NPQ experiments were repeated 3 times.

The de-epoxidation of the xanthophyll cycle pigment Dd during excess PAR and PAR+UVR was studied in low and high light acclimated cultures. Exponentially growing cells were transferred to quartz cuvettes and exposed to simulated surface irradiance as described for the field experiments. Dd de-epoxidation was assessed for 15 ml samples that were obtained after 20, 60, 120, and 200 min of simulated surface irradiance.

Samples were filtered through 25 mm GF/F filters (Whatman) under low vacuum, snap frozen in liquid nitrogen, and stored at −80°C until processing. Sampling took <2 min, thereby avoiding rapid changes in xanthophyll cycle pigments. The experiments were repeated 4 to 6 times for each species and light condition.

Analytical procedures. ***NPQ measurements:*** In the field experiments, 30 ml samples were collected from the cuvettes by a syringe and injected into the flow-through measuring cuvette of a pulse amplitude modulated fluorometer (WATER-PAM, Walz). For the lab cultures, 5 ml samples were used. Measurements were performed before and after 20 min PAR and PAR+UVR, and during recovery (90 min) in low light over 10 min intervals. Terminology of fluorescence parameters is according to Maxwell & Johnson (2000) F'_m was determined after a saturating light pulse (0.8 s, 4000 µmol photons m^{-2} s^{-1}) and F'_v/F'_m was calculated from the basal fluorescence (F'_0) and F'_m: $F'_v/F'_m = (F'_m \times F'_0)/F'_m$. A new sample was used for each measurement. The instrument settings were not changed during the experiment and filtered sea water was used to zero the instrument. A 120 ml phytoplankton sample was dark-adapted in the same set-up for 90 min to determine F^0_m and F_0, from which the maximum dark-adapted quantum yield (F_v/F_m) was determined. NPQ of chlorophyll fluorescence was calculated from the measurements after dark adaptation and from those during recovery after excess radiation according to Bilger & Björkman (1990): $NPQ = (F^0_m - F'_m)/F'_m$. We distinguished between slow (>40 min) and fast (0 to 40 min) relaxing NPQ components (Walters & Horton 1991). The slow component (NPQ_S) is assumed to represent repair of PSII damage, since slow relaxing zeaxanthin quenching is not present in the investigated algal species. The fast component (NPQ_F) is assumed to represent relaxation of xanthophyll cycle quenching. State transitions that also have a short relaxation time have not been reported for the investigated species. NPQ_S and NPQ_F were calculated according to Maxwell & Johnson (2000): $NPQ_S = (F^0_m - F^r_m)/F^r_m$, and $NPQ_F = (F^0_m/F'_m) - (F^0_m/F^r_m)$. Because significant F_0 quenching was observed in most samples, F^r_m was calculated from F'_v (= $F'_m - F'_0$) of the last part of the relaxation curve, which is more accurate than F'_m (Roháček 2010). Log-transformed F'_v from 40 to 90 min recovery was plotted against time. F'_v was extrapolated by linear regression back to the time when simulated surface irradiance exposure ended. By adding F_0 to this value the F^r_m was calculated. The F^r_m represented F'_m that would have been measured directly after exposure if only the slow relaxing component was present. For this calculation it is assumed that F_0 quenching is attributed to NPQ_F. Total NPQ was calculated as NPQ_S + NPQ_F, which equals the NPQ directly after excess irradiance: $(F^0_m - F'_m)/F'_m$.

Pigments: Filters were freeze dried for 48 h and extracted in 5 ml acetone (90% v/v) for 48 h in darkness at 4°C. Pigments were separated on a Waters 960 HPLC system with a C_{18} 5 µm DeltaPak reversed phase column (Waters) and identified using retention time and diode array detection at 436 nm. The HPLC was calibrated against standards obtained from DHI LAB Products. The contribution of dinoflagellates, cryptophytes, chlorophytes (chlorophytes and prasinophytes were not distinguished), diatoms, haptophytes (haptophyte types 6 and 8 were pooled), and cyanobacteria was estimated using the CHEMTAX 1.95 program (Mackey et al. 1996). Using pigment ratios relative to chl *a* for the Southern Ocean phytoplankton, this program applies a steepest descent algorithm to estimate the contribution of taxonomic groups to the chl *a* concentration. The same pigment ratios were applied for samples from the chl maximum and below the chl maximum. The pigments applied in CHEMTAX were chl c_3, 19′-butanoyloxyfucoxanthin, fucoxanthin, 19′-hexanoyloxyfucoxanthin, peridinin, alloxanthin, violaxanthin, zeaxanthin, antheraxanthin, lutein, chl *a* and chl *b*.

Xanthophyll de-epoxidation state was determined as Dt relative to the sum of Dd and Dt. The photoprotective pigment ratio was calculated as the sum of Dd and Dt relative to chl *a*.

POC: Filters were acidified for 4 h by fuming HCl (37% v/v), dried at 60°C overnight, folded in tin capsules, and measured on a nitrogen and carbon analyzer (Flash EA™ 1112, Interscience).

Statistics: Total NPQ, and contributions of NPQ_S and NPQ_F after PAR and PAR+UVR from different sampling stations were compared with a multi factor analysis of variance (ANOVA, Statistica 8.0). Hydrographic parameters (chl maximum depth, PAR attenuation, salinity in the upper water column) from S1 and S2 were compared using a single factor ANOVA. These parameters were also tested separately for shared sampling days of S1, S2, and S3 (n = 5). The same was done for CHEMTAX composition of taxonomic groups, photoprotective pigment ratios and NPQ characteristics after excess PAR and UVR. S1 samples from 2 depths (chl maximum and below chl maximum) were compared for 6 shared sampling days (n = 6). The maximum quantum yield of PSII from dark-adapted samples (F_v/F_m) was compared by a single factor ANOVA for S1, S2, and S3. For *Chaetoceros brevis* and *Phaeocystis antarctica* cultures, differences in total NPQ, contributions of NPQ_S and NPQ_F, and xanthophyll cycle pigment de-epoxidation state were tested with a multi factor ANOVA (species, PAR, PAR+UVR). Differences were considered significant at $p < 0.05$.

RESULTS

Hydrographic conditions, phytoplankton distribution, and photoacclimation of field samples

A strong density (calculated as sigma theta) gradient was a persistent feature in CTD profiles from Potter Cove (example Fig. 3). A shallow mixed layer (2 to 28 m) was calculated at all stations (Table 1). Chlorophyll fluorescence profiles in Potter Cove showed a distinct subsurface maximum below the estimated mixed layer. Although S1, S2, and S3 were only a few kilometers apart (Fig. 1), differences in hydrographic conditions were noted. On average, the depth of the chl maximum was significantly shallower in S2 and S3 (10.3 ± 3.2, 9.2 ± 3.9 m) than in S1 (13.9 ± 4.7 m, $p = 0.011$) (Table 1). The PAR attenuation coefficient for S1 and S2 was on average 0.22 and 0.3 m^{-1}, respectively, and the chl maximum was well above the 1% PAR depth. High K_d values (average 0.86 m^{-1}) were found for S3, where the chl maximum was frequently below the 1% PAR depth. There was a significant negative correlation between near-surface salinity (salinity binned for the first 1 to 4 m) and the attenuation coefficient for PAR when comparing data from all stations ($n = 35$, $p = 0.0008$, $R^2 = 0.77$, results not shown). The chl *a* concentration in the chl maximum increased over time, reaching a maximum of 3.2 mg m^{-3} at the beginning of February (Table 1). No clear differences in average chl *a* concentration of the chl maximum were found between sampling locations ($p = 0.07$). Near the water surface, fluorescence suggested lower chl than determined by HPLC (Fig. 3). POC (mg l^{-1}) correlated significantly ($p < 0.001$) with chl *a* concentration ($R^2 = 0.8$, $n = 41$, data from all stations, results not shown). The C:N ratio was on average 4.982 ± 0.436 and did not change significantly over time (data from all stations, results not shown). Differences in the photoprotective pigment ratio were noted between samples from different depths. The photoprotective pigment ratio was significantly lower in S1 samples from below the chl maximum than those from the chl maximum ($p < 0.0001$, Fig. 4C). The photoprotective ratio was not different in S1, S2, and S3 on shared sampling days (Fig. 4C).

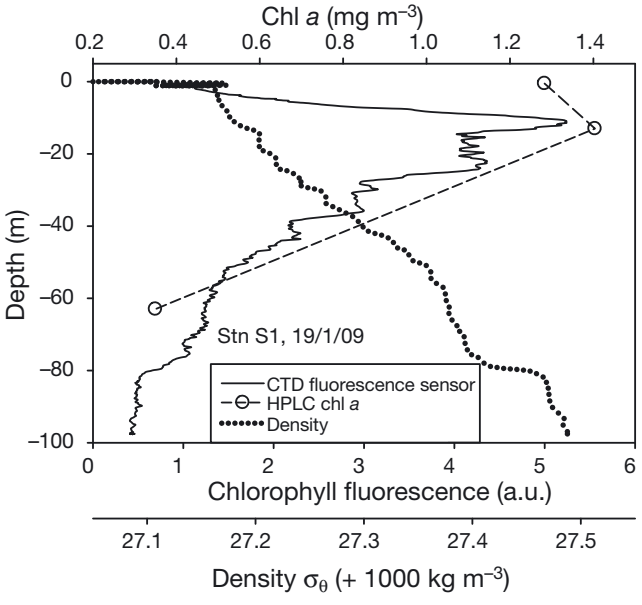

Fig. 3. Chlorophyll fluorescence and density (sigma theta units) profile from a CTD cast in Potter Cove at Stn S1 on 19 January 2009. HPLC determined chl *a* (symbols) is included for 3 depths. Note the deviation between HPLC determined chl *a* and the signal from the fluorescence sensor near the surface

Table 1. Hydrographic data (depth of the euphotic zone, 1% PAR; upper mixed layer, UML; and chl maximum, chl Z_{max}) and the chl *a* concentration in the chl maximum at sampling stations S1, S2 and S3 in Potter Cove, King George Island, Antarctica. nd = not determined

Date (dd/mm/yy)	Depth (m) 1% PAR	Depth (m) UML	Depth (m) Chl_{max}	Chl *a* max. (mg m^{-3})
Stn S1				
15/01/09	30.7	2.7	26.0	0.96
16/01/09	8.0	4.8	10.0	1.03
17/01/09	9.6	28.0	7.4	0.69
19/01/09	23.5	2.1	12.2	1.40
21/01/09	16.9	10.9	11.6	0.86
22/01/09	27.0	2.7	12.4	2.02
23/01/09	30.9	2.1	19.0	1.20
26/01/09	33.7	12.9	17.9	1.84
27/01/09	32.7	2.1	16.3	2.23
28/01/09	31.3	2.1	10.8	2.65
31/01/09	27.6	6.8	7.9	1.86
03/02/09	29.9	4.8	14.5	2.14
04/02/07	28.0	2.7	11.3	2.15
05/02/09	17.5	3.4	12.2	2.06
06/02/09	29.5	2.1	17.1	nd
07/02/09	31.1	2.1	16.1	1.69
Stn S2				
15/01/09	6.6	2.0	12.0	0.76
16/01/09	6.6	2.1	4.5	0.90
19/01/09	18.9	2.1	4.9	nd
21/01/09	23.1	7.5	8.2	0.58
22/01/09	25.3	9.6	12.2	1.05
23/01/09	15.4	2.1	10.0	1.35
26/01/09	22.5	8.9	10.8	1.77
27/01/09	21.2	2.1	8.9	2.68
28/01/09	23.2	2.1	7.2	2.69
31/01/09	17.5	4.1	7.1	3.19
03/02/09	27.5	2.1	16.2	0.96
04/02/09	27.3	8.2	11.9	2.00
05/02/09	16.6	8.2	9.8	2.05
07/02/09	23.5	2.1	15.0	1.77
Stn S3				
27/01/09	3.3	2.1	8.9	2.76
28/01/09	4.3	2.1	5.8	2.67
31/01/09	4.7	2.1	7.3	3.08
04/02/09	8.6	2.1	14.7	1.74
06/02/09	13.9	2.1	6.6	nd

Taxonomic composition based on CHEMTAX

Samples (n = 44) from the chl maximum were dominated by diatoms (Fig. 5). Microscopy revealed the presence of species from the genera *Thalassiosira, Chaetoceros, Corethron,* and *Coscinodiscus*. Diatom abundance increased over time from 66% in January to 78% in the beginning of February, whereas haptophytes (including *Phaeocystis antarctica* flagellates) decreased from 18 to 10% over the same period. This coincided with an increase in 19′-butanoyloxyfucoxanthin at the expense of 19′-hexanoyloxyfucoxanthin. Below the chl maximum (S1), haptophytes (37 ± 14%) were significantly more abundant, whereas diatoms (55 ± 11%) were lower, compared to samples from the chl maximum (p = 0.001, results not shown). Chlorophytes decreased in abundance below the chl maximum from 12 to 3%, whereas dinoflagellates and cryptophytes were present in low relative amounts (3 to 1%). Taxonomic composition in the chl maximum as calculated by CHEMTAX was not significantly different between S1, S2 and S3 on shared sampling days (p = 0.5).

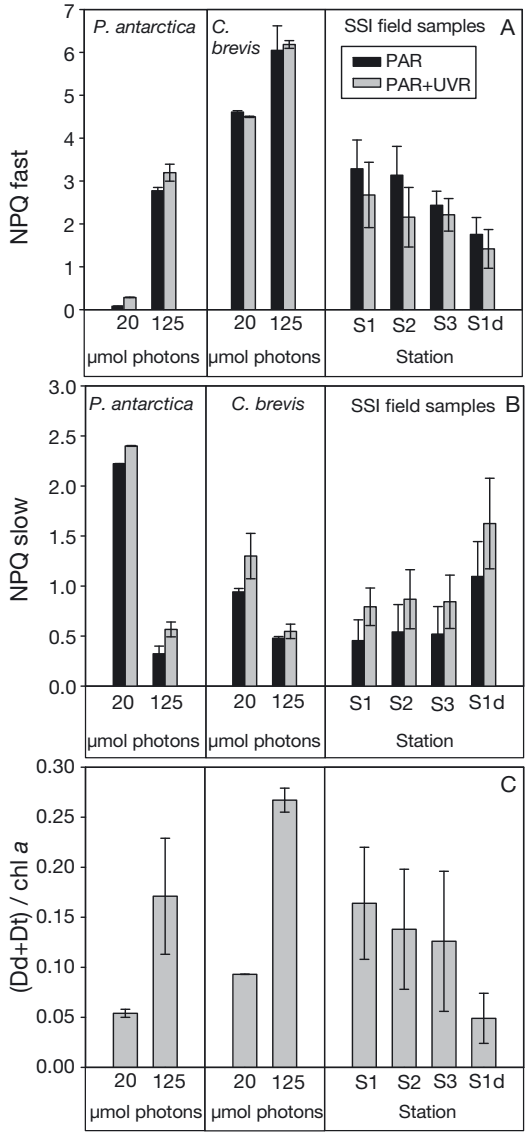

Fig. 4. (A) Fast relaxing non-photochemical quenching (NPQ), (B) slow relaxing NPQ and (C) photoprotective pigment ratio (sum of diadinoxanthin and diatoxanthin relative to chl *a*), derived from recovery data in low light after 20 min simulated surface irradiance (PAR, PAR+UVR) for low (20 µmol photons) and high (125 µmol photons) light acclimated *Phaeocystis antarctica*, *Chaetoceros brevis*, and for chlorophyll maximum samples from Stns S1, S2, S3, and from S1 below the chlorophyll maximum (S1d). Data are mean ± SD for 4 replicates for the cultures, and 14, 12, 4, and 6 replicates for S1, S2, S3, and S1d, respectively

Maximum quantum yield of PSII

Average dark-adapted maximum quantum yield of PSII (F_v/F_m) in the chl maximum samples decreased over time from 0.684 (±0.06) to 0.599 (±0.03). The highest values were recorded in samples from below the chl maximum from S1 (average F_v/F_m: 0.706 ± 0.09) (results not shown).

Field experiments

NPQ of field samples after simulated surface irradiance

Exposure for 20 min to PAR and PAR+UVR caused a strong reduction of the photosynthetic yield of PSII (Fig. 6) and a strong induction of NPQ. Total NPQ (on average 3.3 ± 0.7, n = 62) was significantly lower after PAR+UVR (3.2 ± 0.7) than after PAR (3.5 ± 0.7, p = 0.002). This effect was caused by stronger F_0 quenching after PAR than after PAR+UVR. Total NPQ (2.9 ± 0.6) was significantly lower for S1 samples from below the chl maximum compared to S1 chl maximum samples. NPQ_F was always dominant in samples from S1, S2, and S3, but was significantly (p < 0.0001) lower after PAR+UVR (72.9 ± 9.2%, n = 31) than after PAR (85.8 ± 6.6%) (Fig. 4). Conversely, the slow relaxing component comprised a significantly larger part of total NPQ after PAR+UVR (27.1 ± 0.7%), compared to PAR (14.2 ± 0.7%) (Fig. 4). The contribution of NPQ_S was significantly higher (p < 0.0001) for S1 samples from below the chl maximum (40 to 83 m depth) (38.1 ± 11.0 and 53.4 ± 9.5% for PAR and PAR+UVR, respectively, n = 6) than that from the chl maximum of S1 and S2 on shared sampling days. No significant differences in the contribution of slow and fast NPQ components were found between S1, S2, and S3 on shared sampling days (n = 4 to 14, p = 0.4).

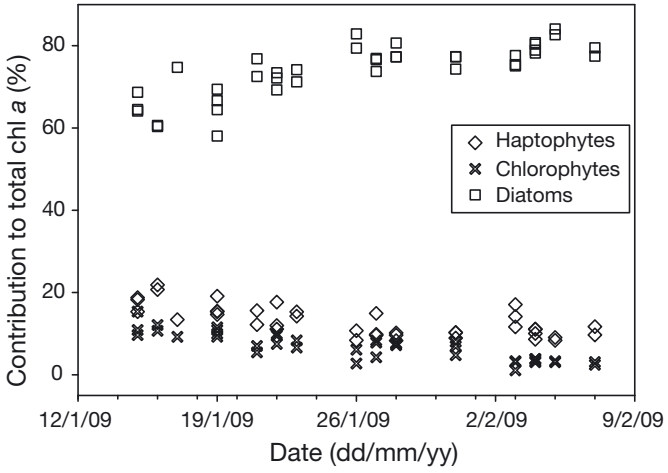

Fig. 5. Taxonomic composition calculated from pigment composition using CHEMTAX, showing the 3 major taxonomic groups (diatoms, haptophytes, and chlorophytes) from the chlorophyll maximum samples from Stns S1, S2, and S3 in Potter Cove in January and February 2009. Taxonomic composition is expressed as contribution (%) to the chl *a* concentration. Samples from below the chlorophyll maximum at S1 are not shown

Bag experiments: NPQ

The bags that received 9% radiation for 12 d showed a higher contribution of NPQ_S (PAR: 24%; PAR+UVR: 49%) to total NPQ than those that received 45% radiation for 2 additional days (PAR: 7.1%; PAR+UVR: 15%), when challenged by 20 min simulated surface irradiance (data not shown).

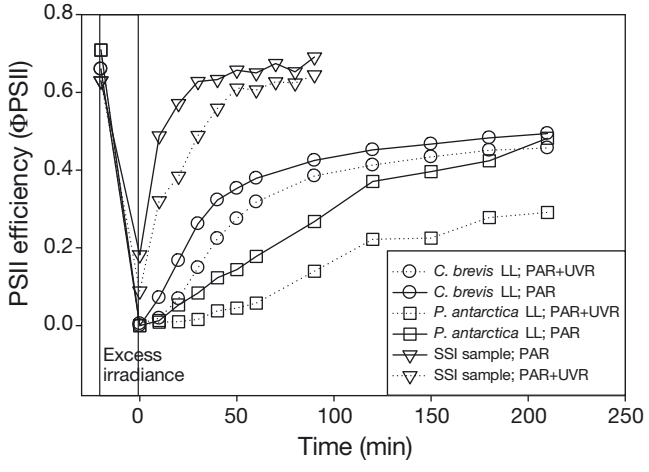

Fig. 6. Photosystem II (PSII) efficiency (quantum yield of PSII) after 20 min simulated surface irradiance (PAR, PAR+UVR) and during recovery in low light (LL) for a field sample from the chlorophyll maximum at S1 (21 January 2009) (triangles), and low light acclimated *Chaetoceros brevis* (circles) and *Phaeocystis antarctica* (squares)

Bag experiments: xanthophyll de-epoxidation state during simulated surface irradiance

After 2 wk under 9% light, the chl *a* concentration in the bags (46.5 ± 3.7 mg m^{-3}, 3 bags, 42 samples in total) allowed the investigation of the xanthophyll cycle during simulated surface irradiance. The algal assemblages showed significant Dd de-epoxidation during simulated surface irradiance (Fig. 7C). De-epoxidation of Dd continued during 120 min exposure. Significant differences between PAR and PAR+UVR were not observed with respect to Dd de-epoxidation. The algal assemblages from the bags that were exposed to 45% of ambient light for 2 d showed significantly higher de-epoxidation compared to the 9% light exposed assemblages (Fig. 8). The relaxation of the xanthophyll cycle (Dt epoxidation) in low light was completed within 40 min after simulated surface irradiance (Fig. 8). The photoprotective pigment ratio increased significantly from 0.06 ± 0.008 to 0.18 ± 0.003 after transition from 9 to 45% light, respectively ($p < 0.0001$) (results not shown). Violaxanthin, antheraxanthin, and zeaxanthin were detected in low amounts (18 times lower concentration than Dd and Dt) and were not further considered.

Lab experiments

Maximum quantum yield of PSII, F_v/F_m, was higher after low light compared to high light acclimation for both species (low light: 0.659 ± 0.002 and 0.702 ± 0.01; high light: 0.495 ± 0.004 and 0.573 ± 0.04; for *Chaetoceros brevis* and *Phaeocystis antarctica*, respectively, n = 5 to 8). $F_v/F_m$was significantly higher in *P. antarctica* for both light conditions.

NPQ after simulated surface irradiance

Total NPQ after 20 min simulated surface irradiance was significantly (multi factor ANOVA $p < 0.0001$) higher for the diatom *Chaetoceros brevis* compared to the haptophyte *Phaeocystis antarctica* (Fig. 4). High light acclimated cultures of both species showed significantly more NPQ than low light acclimated cultures ($p < 0.0001$). NPQ total after PAR+UVR and PAR was not different for *P. antarctica* and *C. brevis*.

Significant differences were found in slow and fast relaxing components of total NPQ due to low and high light acclimation and between *Chaetoceros brevis* and *Phaeocystis antarctica*. Low light acclimated *C. brevis* displayed significantly more NPQ_F than low light acclimated *P. antarctica* ($p < 0.0001$). NPQ_F was significantly higher in high light than in low light

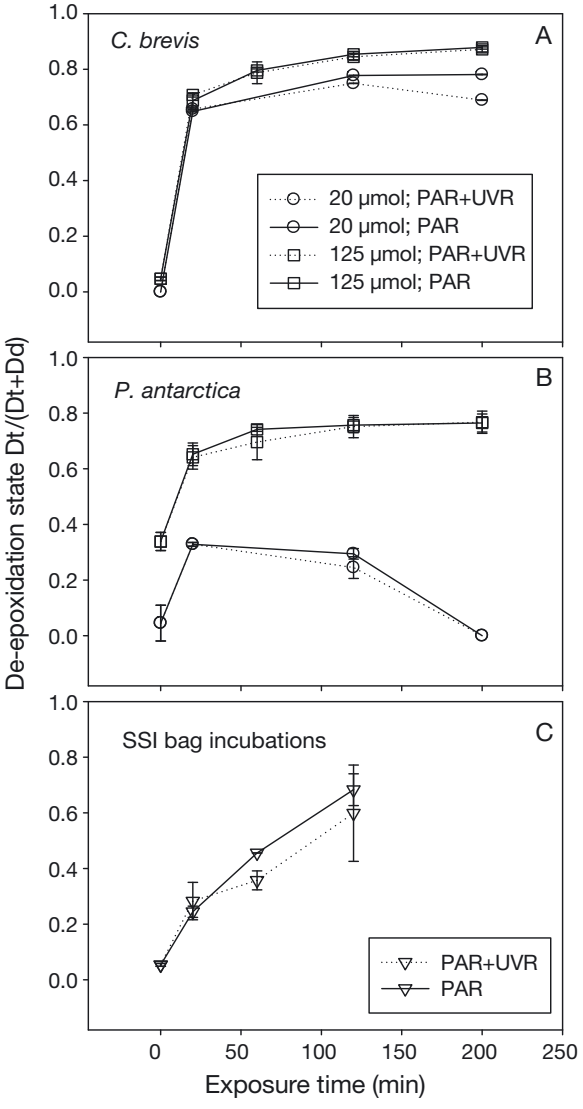

Fig. 7. De-epoxidation state of the xanthophyll cycle pigment diadinoxanthin during simulated surface irradiance (PAR, PAR+UVR) of low (20 µmol photons) and high (125 µmol photons) light acclimated (A) *Chaetoceros brevis* and (B) *Phaeocystis antarctica*, and (C) that of field samples grown in transparent bags for 2 wk under 9% irradiance. Data are mean ± SD for 4 to 6 replicates for the cultures and 2 replicates for the field samples. After 200 min exposure no pigments were detected in low light acclimated *P. antarctica*

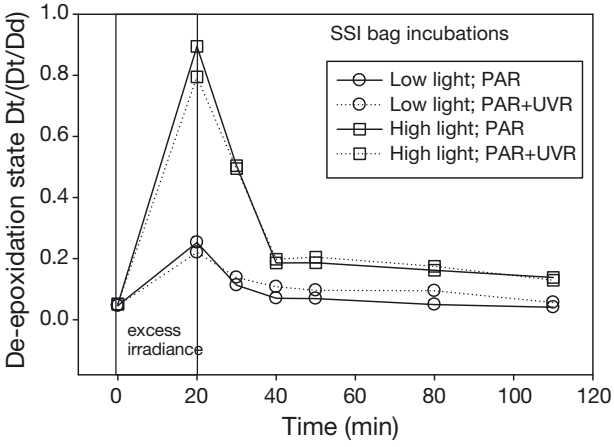

Fig. 8. De-epoxidation state of the xanthophyll cycle pigment diadinoxanthin after 20 min simulated surface irradiance (PAR, PAR+UVR) and during recovery in low light for field samples grown in transparent bags for 2 wk under 9% irradiance (low light) and those that were exposed for 2 additional days to 45% irradiance (high light)

acclimated cultures of both species ($p < 0.0001$). After low light acclimation NPQ_S in *P. antarctica* contributed on average 94.1 ± 4.0% to total NPQ, whereas this was 20.9 ± 4.2% for *C. brevis*. Relative contributions of NPQ_S were 6.6 ± 1.9 and 13.5 ± 2.9% for *C. brevis* and *P. antarctica* respectively after high light acclimation. Relative contributions of NPQ_F and NPQ_S were not different after PAR+UVR and PAR for both species.

Pigment composition

Distinct differences in pigment composition were found between low and high light grown *Chaetoceros brevis* and *Phaeocystis antarctica* (Fig. 4C). Xanthophyll cycle pigments relative to chl *a* (photoprotective pigment ratio) were significantly enhanced in both species under 125 µmol photons m^{-2} s^{-1}, compared to 20 µmol photons m^{-2} s^{-1}. The photoprotective pigment ratio was higher in *C. brevis* than in *P. antarctica* under low (0.093 ± 0.0001 and 0.054 ± 0.004) and high light (0.267 ± 0.012 and 0.171 ± 0.058, respectively). This was most pronounced under low light, where *C. brevis* contained almost 2 times more xanthophyll cycle pigments relative to chl *a* than *P. antarctica* (Fig. 4). In *C. brevis* (20, 125 µmol photons m^{-2} s^{-1}) and *P. antarctica* (125 µmol photons m^{-2} s^{-1}) there was a significant increase (on average 17%) in the photoprotective pigment ratio after 200 min simulated surface irradiance (results not shown).

Dd de-epoxidation during simulated surface irradiance

Simulated surface irradiance for 20 min caused significant Dd de-epoxidation in *Chaetoceros brevis* and *Phaeocystis antarctica* (Fig. 7A,B). Dd de-epoxidation characteristics in low and high light *C. brevis* were comparable, whereas clear differences were observed between low and high light acclimated *P. antarctica*. Low light acclimated *P. antarctica* showed reduced Dd de-epoxidation in simulated surface irradiance. After 200 min PAR+UVR pigments could not be detected in

low light acclimated *P. antarctica* cultures. High light acclimated *P. antarctica* showed similar Dd de-epoxidation characteristics compared to *C. brevis*, but initial de-epoxidation was higher. UVR effects on Dd de-epoxidation were not found during 200 min simulated surface irradiance.

DISCUSSION

The Dd-Dt cycle was the major xanthophyll cycle in field samples as well as in *Chaetoceros brevis* and *Phaeocystis antarctica*. Because the abundance of these pigments depends on the experienced light, comparing the ratio of xanthophyll cycle pigments relative to chl *a* (the photoprotective pigment ratio) could provide information on phytoplankton photoacclimation. The photoprotective pigment ratios of chl maximum samples were in the range of high light (125 µmol photons m^{-2} s^{-1}) acclimated *C. brevis* and *P. antarctica*. Due to strong light attenuation in these coastal waters (average K_d for S1, S2, S3 was 0.22, 0.30, and 0.86 m^{-1}, respectively) the chl maximum experienced on average 4.9, 4.6, and 0% of the incoming light for S1, S2 and S3, respectively. For S1 and S2 this corresponded with a maximum light intensity of around 140 µmol photons m^{-2} s^{-1} at noon. The stabilized water column due to the observed strong density gradient allowed phytoplankton to grow close to the water surface, where it acclimated to relatively high light, explaining the resemblance with high light acclimated cultures.

Not surprisingly, NPQ_F dominated in all chl maximum samples when exposed to excess light, comprising on average 80% of total NPQ. NPQ_F and NPQ_S of field samples were in the range of low light (20 µmol photons m^{-2} s^{-1}) acclimated *Chaetoceros brevis* and high light (125 µmol photons m^{-2} s^{-1}) acclimated *Phaeocystis antarctica*. Nevertheless, the maximum quantum yield (F_v/F_m) of the field samples was higher than that of high light acclimated *C. brevis* and *P. antarctica*. Thus, the chl maximum samples shared characteristics of high and low light acclimation. These differences may be attributed to the light fluctuations experienced in the field (MacIntyre et al. 1996, Van de Poll et al. 2007, Kropuenske et al. 2009), or alternatively, may be caused by species-specific differences in photoacclimation.

Although NPQ_F dominated, a significant part (on average 20%) of NPQ from the chl maximum samples was in the slowly relaxing form after 20 min simulated surface irradiance, whereas significant NPQ_S was also induced in high light acclimated *Phaeocystis antarctica* and *Chaetoceros brevis*. Excess PAR and UVR effects on photosynthesis are minimized but not entirely prevented by high light acclimation (Sobrino et al. 2005, Van de Poll et al. 2010). Relaxation of NPQ_S has been attributed to repair of damaged PSII reaction centers. In the present study, Dt epoxidation (relaxation of NPQ_F) in field samples from the chl maximum appeared to be completed in 40 min, whereas complete PSII recovery took 1 h or longer. NPQ_S increased due to UVR exposure in field samples. This is in line with the observation that UVR increases PSII damage (Hazzard et al. 1997, Bouchard et al. 2005, 2006). The applied UVR was relatively high, and particularly UVBR can be considered as the upper exposure limit for phytoplankton near the water surface. However, significant UVR effects on xanthophyll cycle de-epoxidation state and NPQ were not found over a 200 min exposure period for lab cultures, which was sufficient to induce complete photodegradation of pigments in low light acclimated *P. antarctica*. Total NPQ from the field samples was slightly reduced in response to PAR+UVR, whereas this was not found for the lab cultures. UVBR causes reduced xanthophyll cycle activity in the diatom *Phaeodactylum tricornutum* (Mewes & Richter 2002). Because NPQ total and the contribution of NPQ_S and NPQ_F of field samples and cultures responded differently to UVR, this issue remains unresolved.

We further showed differences in the capacity to deal with periodic excess PAR and UVR between *Phaeocystis antarctica* and *Chaetoceros brevis*. The diatom showed an increased capacity for NPQ_F compared to *P. antarctica,* in concert with higher xanthophyll cycle pigments. Differences between *C. brevis* and *P. antarctica* were most pronounced in low light acclimated cultures. Low light acclimated *P. antarctica* contained less xanthophyll cycle pigments per chl *a* than low light acclimated *C. brevis*, and showed a highly reduced capacity for NPQ_F. Comparable results were found for NPQ in *P. antarctica* and the diatom *Fragilariopsis cylindrus* (Kropuenske et al. 2009). Using a protein synthesis inhibitor, this study also showed that *P. antarctica* relied more strongly on chloroplast protein synthesis to maintain photosynthesis than the diatom *F. cylindrus* (Kropuenske et al. 2009, Mills et al. 2010). In the Ross Sea, *P. antarctica* is abundant in deeply mixed waters, whereas diatom abundance is associated with a stratified water column (Arrigo et al. 1999). Similarly, flagellates dominated over diatoms in deeply mixed stations in Admiralty Bay, King George Island (Kopczynska 1992). The observed differences in photoprotective capacity between diatoms and haptophytes may have caused the diatom dominance during the stratified late summer water column conditions in Potter Cove. Moreover, samples from below the chl maximum were enriched in haptophytes. When exposed to simulated surface irradiance, these samples induced significantly

less total NPQ, with a stronger NPQ_S component compared to those from the chl maximum of S1 and S2. This coincided with a lower photoprotective pigment ratio for the deep samples than those from the chl maximum, comparable to that of low light acclimated *P. antarctica*.

Biomass reached 25-fold higher concentrations when cultivated in transparent plastic bags than in the shallow chl maximum. The bags received 9% of the incoming light, which was higher than the average light experienced at the chl maximum depth (4.6% for S1 and S2). Nevertheless, the algal samples from the bags showed characteristics of low light acclimation, in contrast to those from the chl maximum, possibly caused by shading from high biomass and from sediments in the set-up. Luxurious phytoplankton growth in cultured water samples from the SSI area has previously been described (Schloss et al. 2002, Helbling et al. 1995, Agustí & Duarte 2000) and demonstrates the enormous potential for phytoplankton growth of these waters in terms of available nutrients. Although we did not work in a trace metal free environment and iron was not measured in this study, iron availability is believed not to limit phytoplankton growth in the coastal waters of the SSI (Hewes et al. 2008). This was confirmed by the high maximal quantum yield of PSII (F_v/F_m) of the field samples, because F_v/F_m is one of the first parameters that is affected by iron limitation, before growth rates start to decrease (Greene et al. 1992, van Oijen et al. 2004b).

Since there was no evidence for resource limitation apart from light, phytoplankton growth was constrained either by physical (unfavorable hydrographic conditions) or biological factors (grazing). With regard to photoinhibition, we showed that this is likely to occur near the water surface. The phytoplankton in the shallow chl maximum was dominated by diatoms, which were shown to have a high photoprotective capacity. This does not prevent photoinhibition during excess irradiance, but enhances recovery under favorable irradiance conditions and survival after prolonged excess irradiance exposure. This flexibility is obviously an advantage during frequent excess irradiance exposure. HPLC determined chl *a* from the chl maximum and occasional surface samples were not much different, whereas the CTD fluorescence sensor indicated 5-fold lower concentrations. PAM fluorescence measurements showed that 20 min simulated surface irradiance reduced background fluorescence (F_0) on average to 58% of the maximum value. Assuming that depressed fluorescence of the CTD sensor can be attributed to NPQ, algal excess radiation effects on photosynthesis were detectable in the upper 10 m of the water column. Furthermore, direct F_v/F_m measurements (no dark adaptation) on board revealed low F_v/F_m (~0.2) near the surface, increasing to near maximal values (0.6) around 10 m depth (results not shown). A strong gradient in PSII fluorescence parameters in the upper part of the water column was previously reported for oligotrophic open ocean stations (Raateoja et al. 2009).

Due to the stabilized water column, wind mediated vertical mixing appeared to be confined to the upper meters during the late summer conditions in Potter Cove. Because the depth of the mixed layer affects phytoplankton photoacclimation, photoinhibition will be more pronounced in low light acclimated phytoplankton from deeper mixed layers than those observed for Potter Cove. Accordingly, it was found that UVBR effects were more pronounced in open ocean phytoplankton samples than in samples from coastal Antarctic waters (Fritz et al. 2008). However, such differences are most likely explained by a combination of factors governed by nutrient and light conditions: species composition, photoacclimation (present study), and also the size of the phytoplankton species (Key et al. 2010).

Despite the small spatial scale, considerable variation was observed in salinity, temperature, and PAR attenuation in the upper water layer between sampling stations. PAR attenuation was variable (K_d PAR range: 0.1 to 1.2 m^{-1}) due to periodically high sediment concentrations, caused by glacial meltwater influx. However, significant differences were not found in photoprotective pigment ratios and NPQ between samples from S1, S2, and S3, and no significant differences in taxonomic composition were noted between stations in Potter Cove. Therefore, the variable light conditions at S3 did not cause consistent differences in phytoplankton photoacclimation. Furthermore, the residence time under low irradiance conditions at S3 was not enough to create regional differences in dominant taxonomic groups. The elevated temperature during the past decades has increased meltwater influx and sediment loads in the West Antarctic Peninsula area and also in Potter Cove (Schloss et al. 2008, Schofield et al. 2010). In this respect, and in agreement with previous work, our research shows that 2 effects can be distinguished: stratification of the water column, which potentially enhances phytoplankton growth, and locally high sediment loads that reduce phytoplankton growth due to strong light attenuation (S3).The hydrographic conditions in S1 and S2 favored phytoplankton growth, although this was probably also moderated by the influx of sediment and by photoinhibition near the surface. Currents continuously transport phytoplankton from Potter Cove into the Bransfield Strait, where suspended sediments are lower and the density gradient is diluted. How far the stabilizing influence of fresh water from the SSI extends into Bransfield Strait in

unknown. Assessment of this effect would require collection of phytoplankton and hydrographic data on a broader spatial and temporal scale.

Acknowledgements. We thank the diving team and staff from the Dallmann Laboratory and the Argentinean Jubany station for their help. In addition, we thank S. Crayford for POC analysis, and G. Kulk for assistance with NPQ measurements. This work was funded by the Netherlands Organization for Scientific Research (NWO grant 851.20.032).

LITERATURE CITED

Agustí S, Duarte CM (2000) Experimental induction of a large phytoplankton bloom in Antarctic coastal waters. Mar Ecol Prog Ser 206:73–85

Alderkamp AC, de Baar HJW, Visser RJW, Arrigo KR (2010) Can photoinhibition control phytoplankton abundance in deeply mixed water columns of the Southern Ocean? Limnol Oceanogr 55:1248–1264

Arrigo KR (1994) Impact of ozone depletion on phytoplankton growth in the Southern Ocean: large-scale spatial and temporal variability. Mar Ecol Prog Ser 114:1–12

Arrigo KR, Robinson DH, Worthen DL, Dunbar RD, DiTullio GR, VanWoert M, Lizotte MP (1999) Phytoplankton community structure and the drawdown of nutrients and CO_2 in the Southern Ocean. Science 283:365–367

Bilger W, Björkman O (1990) Role of the xanthophyll cycle in photoprotection elucidated by measurements of light-induced absorbance changes, fluorescence, and photosynthesis in leaves of *Hedera canariensis.* Photosynth Res 25:173–185

Blain S, Quéguiner B, Armand L, Belviso S and others (2007) Effect of natural iron fertilization on carbon sequestration in the Southern Ocean. Nature 446:1070–1074

Bouchard JN, Campbell DA, Roy S (2005) Effect of UV-B radiation on the D1 protein repair cycle of natural phytoplankton communities from three latitudes (Canada, Brazil, and Argentina). J Phycol 41:273–286

Bouchard JN, Roy S, Campbell DA (2006) UVB effects on the photosystem II-D1 protein of phytoplankton and natural phytoplankton communities. Photochem Photobiol 82: 936–951

Buma AGJ, Visser RJW, Van de Poll WH, Villafane V, Janknegt PJ, Helbling EW (2009) Wavelength dependent xanthophyll cycle activity in marine microalgae exposed to natural ultraviolet radiation. Eur J Phycol 44:515–524

De Baar HJW, Boyd P, Coale KH, Landry MR and others (2005) Synthesis of iron fertilization experiments: from the iron age to the age of enlightment. J Geophys Res 110: C09S16, doi: 10.1029/2004JC002601

Dierssen HM, Smith RC, Vernet M (2002) Glacial meltwater dynamics in coastal waters west of the Antarctic peninsula. Proc Natl Acad Sci USA 99:1790–1795

Dimier C, Giovanni S, Ferdinando T, Brunet C (2009) Comparative ecophysiology of the xanthophyll cycle in six marine phytoplanktonic species. Protist 160:397–411

Fritz JJ, Neale PJ, Davis RF, Peloquin JA (2008) Response of Antarctic phytoplankton to solar UVR exposure: inhibition and recovery of photosynthesis in coastal and pelagic assemblages. Mar Ecol Prog Ser 365:1–16

Goss R, Jakob T (2010) Regulation and function of xanthophyll cycle-dependent photoprotection in algae. Photosynth Res 106:103–122

Goss R, Ann Pinto E, Wilhelm C, Richter M (2006) The importance of a highly active and ΔpH-regulated diatoxanthin epoxidase for the regulation of the PSII antenna function in diadinoxanthin cycle containing algae. J Plant Physiol 163:1008–1021

Greene RM, Geider RJ, Kolber Z, Falkowski PG (1992) Iron-induced changes in light harvesting and photochemical energy conversion processes in eukaryotic marine algae. Plant Physiol 100:565–575

Hazzard C, Lesser MP, Kinzie RA III (1997) Effects of ultraviolet radiation on photosynthesis in the subtropical marine diatom, *Chaetoceros gracilis* (Bacillariophyceae). J Phycol 33:960–968

Helbling EW, Villafane VE, Holm-Hansen O (1995) Variability of phytoplankton distribution and primary production around Elephant Island, Antarctica during 1990-1993. Polar Biol 15:233–246

Hewes CD, Reiss CS, Kahru M, Mitchell BG, Holm-Hansen O (2008) Control of phytoplankton biomass by dilution and mixed layer depth in the western Weddell-Scotia confluence. Mar Ecol Prog Ser 366:15–29

Hewes CD, Reiss CS, Holm-Hansen O (2009) A quantitative analysis of sources for summertime phytoplankton variability over 18 years in the South Shetland Islands (Antarctica) region. Deep-Sea Res I 56:1230–1241

Key T, McCarthy A, Campbell DA, Six C, Roy S, Finkel ZV (2010) Cell size trade-offs govern light exploitation strategies in marine phytoplankton. Environ Microbiol 12: 95–104

Kopczynska EE (1992) Dominance of microflagellates over diatoms in the Antarctic areas of deep vertical mixing and krill content stations. J Plankton Res 14:1031–1045

Kropuenske LR, Mills MM, van Dijken GL, Bailey S, Robinson DH, Welschmeyer NA, Arrigo KR (2009) Photophysiology in two major Southern Ocean phytoplankton taxa: Photoprotection in *Phaeocystis antarctica* and *Fragillariopsis cylindrus.* Limnol Oceanogr 54:1176–1196

Larkum AWD, Karge M, Reifarth F, Eckert HJ, Post A, Renger G (2001) Effect of monochromatic UV-B radiation on electron transfer reactions of Photosystem II. Photosynth Res 68:49–60

Lavaud J, Strzepek RF, Kroth PG (2007) Photoprotection capacity differs among diatoms: possible consequences on spatial distribution of diatoms related to fluctuations in the underwater light climate. Limnol Oceanogr 52:1188–1194

MacIntyre HL, Geider RJ, McKay RM (1996) Photosynthesis and regulation of rubisco activity in net phytoplankton from Delaware Bay. J Phycol 32:718–731

Mackey MD, Mackey DJ, Higgins HW, Wright SW (1996) CHEMTAX — a program for estimating class abundances from chemical markers: application to HPLC measurements of phytoplankton. Mar Ecol Prog Ser 144:265–283

Maxwell K, Johnson GN (2000) Chlorophyll fluorescence — a practical guide. J Exp Bot 51:659–668

Mewes H, Richter M (2002) Supplementary ultraviolet-B radiation induces a rapid reversal of the diadinoxanthin cycle in the strong light-exposed diatom *Phaeodactylum tricornutum.* Plant Physiol 130:1527–1535

Mills MM, Kropuenske LR, van Dijken GL, Robinson DH and others (2010) Photophysiology in two major Southern Ocean phytoplankton taxa: Photosynthesis and growth of *Phaeocystis antarctica* (Prymnesiophyceae) and *Fragilariopsis cylindrus* (Bacillariophyceae) under simulated mixed-layer irradiance. J Phycol 46:1114–1127

Raateoja M, Mitchell BG, Wang H, Olivo E (2009) Effect of water column light gradient on phytoplankton fluorescence transients. Mar Ecol Prog Ser 376:85–101

Roháček K (2010) Method for resolution and quantification of

components of the non-photochemical quenching (q_N). Photosynth Res 105:101–113

Schloss IR, Ferreyra GA (2002) Primary production, light and vertical mixing in Potter Cove, a shallow bay in the maritime Antarctic. Polar Biol 25:41–48

Schloss IR, Ferreyra GA, Ruiz-Pino D (2002) Phytoplankton biomass in Antarctic shelf zones: a conceptual model based on Potter Cove, King George Island. J Mar Syst 36:129–143

Schloss IR, Ferreyra GA, González O, Atencio A and others (2008) Long-term hydrographic conditions and trends in Potter Cove. Rep Polar Mar Res 571:382–389

Schofield O, Ducklow HW, Martinson DG, Meredith MP, Moline MA, Fraser WR (2010) How do polar marine ecosystems respond to rapid climate change? Science 328: 1520–1523

Sobrino C, Neale PJ, Montero O, Lubián LM (2005) Biological weighting function for xanthophyll de-epoxidation induced by ultraviolet radiation. Physiol Plant 125:41–51

Strzepek RF, Harrison PJ (2004) Photosynthetic architecture differs in coastal and oceanic diatoms. Nature 431: 689–692

Van de Poll WH, Buma AGJ (2009) Does ultraviolet radiation affect the xanthophyll cycle in marine phytoplankton? Photochem Photobiol Sci 8:1295–1301

Van de Poll WH, Alderkamp AC, Janknegt PJ, Roggeveld J, Buma AGJ (2006) Photoacclimation modulates excessive photosynthetically active and ultraviolet radiation effects in a temperate and Antarctic marine diatom. Limnol Oceanogr 51:1239–1248

Van de Poll WH, Visser RJW, Buma AGJ (2007) Acclimation to a dynamic irradiance regime changes excessive irradiance sensitivity of *Emiliania huxleyi* and *Thalassiosira weissflogii*. Limnol Oceanogr 52:1430–1438

Van de Poll WH, Buma AGJ, Visser RJW, Janknegt PJ, Villavañe VE, Helbling EW (2010) Xanthophyll cycle activity and photosynthesis of *Dunaliella tertiolecta* (Chlorophyceae) and *Thalassiosira weissflogii* (Bacillariophyceae) during fluctuating solar radiation. Phycologia 49: 249–259

van Oijen T, Van Leeuwe MA, Granum E, Weissing FJ, Bellerby RGJ, Gieskes WWC, de Baar HJW (2004a) Light rather than iron controls photosynthate production and allocation in Southern Ocean phytoplankton populations during austral spring. J Plankton Res 26:885–900

van Oijen T, Van Leeuwe MA, Gieskes WWC, de Baar HJW (2004b) Effects of iron limitation on photosynthesis and carbohydrate metabolism in the Antarctic diatom *Chaetoceros brevis* (Bacillariophyceae). Eur J Phycol 39:161–171

Walters RG, Horton P (1991) Resolution of components of non-photochemical chlorophyll fluorescence quenching in barley leaves. Photosynth Res 27:121–133

Editorial responsibility: Hans Heinrich Janssen Oldendorf/Luhe, Germany

Submitted: July 8, 2010; Accepted: December 13, 2010
Proofs received from author(s): March 8, 2011